Journal of Sound and Vibration 333 (2014) 7386–7400

Contents lists available at ScienceDirect

Journal of Sound and Vibration

journal homepage: www.elsevier.com/locate/jsvi

Adaptive bistable stochastic resonance and its application in mechanical fault feature extraction

Yi Qin [a,b,*], Yi Tao [a], Ye He [a], Baoping Tang [a]

[a] State Key Laboratory of Mechanical Transmission, Chongqing University, Chongqing 400044, People's Republic of China
[b] Department of Mechanical Engineering, University of Michigan, Ann Arbor, MI 48109, USA

ARTICLE INFO

Article history:
Received 15 June 2014
Received in revised form
29 July 2014
Accepted 30 August 2014
Handling Editor: L.G. Tham
Available online 22 September 2014

ABSTRACT

Stochastic resonance (SR) is an important approach to detect weak vibration signals from heavy background noise. In order to increase the calculation speed and improve the weak feature detection performance, a new bistable model has been built. With this model, an adaptive and fast SR method based on dyadic wavelet transform and least square system parameters solving is proposed in this paper. By adding the second-order differential item into the traditional bistable model, noise utilization can be increased and the quality of SR output signal can be improved. The iteration algorithm for implementing the adaptive SR is given. Compared with the traditional adaptive SR method, this algorithm does not need to set up the searching range and searching step size of the system parameters, but only requires a few iterations. The proposed method, discrete wavelet transform and the traditional adaptive SR method are applied to analyzing simulated vibration signals and extracting the fault feature of a rotor system. The contrastive results verify the superiority of the proposed method, and it can be effectively applied to weak mechanical fault feature extraction.

1. Introduction

Rotary machinery is one of the most commonly used machines in mechanical engineering, such as compressors, centrifugal pump, motorized spindles and water turbines. Usually, vibration analysis is used for the health monitoring and fault diagnosis of rotating machines, as their vibration signals contain rich mechanical equipment condition information. However, if a rotating machine has an early fault or the working environment is very bad, the faulty vibration signals are often submerged in strong background noise coming from other coupled machine components, measuring instrument and working environment. The strong noise may seriously influence the accuracy of fault diagnosis. Therefore, various signal processing approaches are applied to extract the fault feature from the noise. Recently, overcomplete wavelet transform [1,2], sparse signal processing [3,4], ensemble empirical mode decomposition [5,6], and multicomponent demodulation based on iterative energy separation [7] have been successfully applied to incipient fault identification. Unfortunately, these methods may weaken the useful fault feature while they suppress the noise. Compared with these traditional methods of weak signal detection, stochastic resonance (SR) can take advantage of the noise to enhance the weak signals by some nonlinear systems, thus it is very suitable for weak fault feature extraction. In the past few years, SR has been widely applied

* Corresponding author at: State Key Laboratory of Mechanical Transmission, Chongqing University, Chongqing 400044, People's Republic of China. Tel./fax: +86 23 65105721.
E-mail address: qy_808@aliyun.com (Y. Qin).

http://dx.doi.org/10.1016/j.jsv.2014.08.039
0022-460X/

to rub-impact fault detection of rotor system [8], planetary gearbox fault diagnosis [9], rolling bearing fault diagnosis [10], competitive neural networks [11], etc.

The concept of SR was first put forward by Benzi et al. [12] in their study on the problem of periodically recurrent ice ages. The SR phenomenon has been observed in many bistable systems by physical experiments [13–15]. For a nonlinear bistable system, SR can be realized by adjusting the system parameters or increasing the intensity of the noise. Gang et al. [16] put forward the famous idea of adiabatic approximation theory, which proved that stochastic resonance is used to detect a weak signal. Then Gammaitoni et al. [17] theoretically proved that SR with small parameters could just be driven by very low frequency signal, due to the restriction of the adiabatic approximation or linear theory. Thus, the large parameter SR has been widely researched during the past few years and several improved SR have been proposed. Leng et al. proposed re-scaling stochastic resonance (RFSR) to solve the small parameter problem [18,19]. Mao et al. modulated the measured signal so as to make the SR system meet the adiabatic approximation theory [20]. Combining the two methods, Tan et al. further proposed frequency-shifted and re-scaling stochastic resonance (FRSR) [21]. He et al. developed a method of multiscale noise tuning to realize the SR at a fixed noise level [22]. Except for the small parameter problem, how to obtain optimal SR effect is worth investigating. Recently, Kohar et al. made use of periodic forcing to enhance the SR effect [23]. However, the performance of SR is generally enhanced by adjusting system parameters or by increasing the strength of noise. In some cases, given a definite SR model, increasing the strength of noise may not improve the detection effect of SR, e.g., the analyzed signal has a low signal-to-noise ratio (SNR). Therefore, adjusting system parameters is a better way to enhance the detection performance of SR. Li et al. made use of sliding window and weighted kurtosis to achieve the optimal selection of SR system parameters [24]. Lu et al. achieve adaptive SR of multi-frequency signal by the power spectrum of the output signal that is a measurement index [25]. However, these methods obtain optimal parameters by sequentially searching in a range set in advance. It leads to low computation efficiency, and even the optimal parameters may not be got if the searching range is not correctly chosen. Therefore, it is necessary to research a new adaptive SR method which can automatically calculate the optimal system parameters and do it fast. Moreover, the resonance model has an important influence on the weak feature detection performance of SR. Currently, SR can use the monostable model, the bistable model and the multi-stable model [26,27], in which the bistable model is the most widely used. For a bistable system, there may be several types of models [28,29]. By setting up a new and good bistable resonance model, the capability of extracting the weak feature of bistable SR can be further improved. Therefore, this paper focuses on the study of an adaptive and fast SR method based on a new bistable model, in order to increase the computation speed of searching optimal SR system parameters and improve the detection ability of the SR method for weak signals. First, a second-order differential item is added into the tradtional bistable model, so the new bistable model can further increase the noise utilization and smooth signal. And according to the smoothing effect of wavelet transform, an iterative algorithm based on dyadic wavelet transform and least square system parameters solving method for calculating the optimal system parameters is proposed. With this algorithm, the optimal SR parameters and detection results can be fast obtained after just a few iterative computations. This proposed SR method has a better weak signal detection capability than the traditional bistable SR method and can be effectively applied to weak fault feature extraction in mechanical engineering.

In the following, the bistable SR theory is introduced in Section 2. Then the new bistable model and the iterative algorithm for achieving optimal SR are introduced in Section 3. Section 4 compares the new bistable SR method with the classical bistable SR method and demonstrates its advantage in weak signal detection. The proposed bistable SR method is applied to the fault feature extraction of a rotor system in Section 5, and the results validate its effectiveness and superiority. Finally, this paper is concluded in Section 6.

2. The bistable SR theory

SR is a nonlinear phenomenon in which the weak signal is enhanced, and the noise is weakened through the interaction of the nonlinear system, small parameter signal and noise. It has been proved in many literatures that the nonlinear SR method is effective in weak signal analysis. To describe the SR, the overdamped motion of a Brownian particle in a bistable potential in the presence of noise and periodic/aperiodic force is considered as follows:

$$\frac{\mathrm{d}x}{\mathrm{d}t} = -U'(x) + s(t) + n(t) \tag{1}$$

where $x(t)$ is the system output, $s(t)$ is a periodic/aperiodic signal, $n(t)$ is a Gaussian white noise, $U(x)$ denotes the reflection-symmetrical quartic potential as

$$U(x) = -\frac{a}{2}x^2 + \frac{b}{4}x^4 \tag{2}$$

According to Eq. (2), two stable points are $x_{\pm} = \pm\sqrt{a/b}$ and one critical stable point is $x_0 = 0$. The height of the potential barrier is $\Delta U = a^2/4b$. Substituting Eq. (2) into Eq. (1), we can get

$$\frac{\mathrm{d}x}{\mathrm{d}t} = ax - bx^3 + s(t) + n(t) \tag{3}$$

Let $s(t)=A_0\ \sin(2\pi f_0 t+\varphi)$ and $n=\sqrt{2D}\xi(t)$ with $\langle n(t),n(t+\tau)\rangle=2D\delta(\tau)$, where D is the noise intensity and $\xi(t)$ represents a Gaussian white noise with zero mean and unit variance. Then Eq. (1) can be rewritten as

$$\frac{\mathrm{d}x}{\mathrm{d}t}=ax-bx^3+A_0\ \sin(2\pi f_0 t+\varphi)+\sqrt{2D}\xi(t) \tag{4}$$

where a and b are barrier parameters with positive real values. For the bistable SR model, the output amplitude depends on the noise intensity D, which is given by

$$\bar{x}(D)=\frac{A_0\langle x^2\rangle_0}{D}\frac{r_k}{\sqrt{r_k^2+\pi^2 f_0^2}} \tag{5}$$

where $\langle x^2\rangle_0$ is the D-dependent variance of the stationary unperturbed system ($A_0=0$), and r_k is the Kramers rate. The Kramers rate denotes the transition rate of the Brownian particle caused by noise and can be calculated by using the following formula:

$$r_k=\frac{1}{2\pi}\sqrt{|U''(x_\pm)||U''(x_0)|}\exp\left(\frac{U(x_\pm)-U(x_0)}{D}\right)=\frac{1}{\sqrt{2}\pi}\exp\left(-\frac{\Delta U}{D}\right)=\frac{1}{\sqrt{2}\pi}\exp\left(-\frac{a^2}{4bD}\right) \tag{6}$$

Eq. (5) indicates that the output amplitude first increases with the increasing noise level until reaching a maximum and then decreases again. This process represents the SR phenomenon. The maximum amplitude can be obtained when the following matching relationship is satisfied:

$$\frac{2}{r_k}=\frac{1}{f} \tag{7}$$

Moreover, Eq. (6) indicates that the Kramers rate is determined by noise for a bistable system with constant parameters. Therefore, it can be seen from Eqs. (5) to (7) that the response of the bistable SR system can be manipulated by changing the noise intensity or system parameters.

The basic bistable SR model can be further explained by the Lorentzian distribution property of the power spectral density $S_n(f)$ contributed by the noise [17]. The Lorentzian distribution is characterized by concentrating most of the noise energy into the low frequency region. The energy concentration then induces the SR phenomenon of the low-frequency driving component.

3. Adaptive and fast SR

3.1. The new bistable model

Currently, most papers research the bistable SR method based on the model given by Eq. (1). It can be seen from the viewpoint of signal processing that this model is similar to a first-order low-pass filter. Compared with the conventional filter, the SR method can not only 'filter out' the high-frequency signal, but also enhance the low-frequency signal due to the role of the nonlinear item in the bistable model. It is well known that the filtering performance of a filter can be improved by increasing the filter order. Similarly, in order to further enhance the SR effect, we can increase the order of the bistable model. Thus, a new second-order bistable model is built up, and its governing equation is defined as

$$\frac{\mathrm{d}^2x}{\mathrm{d}t^2}+\frac{\mathrm{d}x}{\mathrm{d}t}=ax-bx^3+s(t)+n(t) \tag{8}$$

where a and b are system parameters, $x(t)$ is the system output, $s(t)$ is the system input and $n(t)$ is a Gaussian white noise. Comparing Eq. (3) with Eq. (8), we can easily see that the potential function remains the same, but a second-order difference item x'' is inserted into the new model. By the use of this second-order difference item x'', noise and glitches can be further removed. It can be proved by the following simulation experiment. To solve the second-order difference equation, Eq. (8) needs to be rewritten as

$$\begin{cases} y=\frac{\mathrm{d}x}{\mathrm{d}t} \\ \frac{\mathrm{d}y}{\mathrm{d}t}=ax-bx^3-y+s(t)+n(t) \end{cases} \tag{9}$$

Then the fourth-order Runge–Kutta method can be used to solve the nonlinear system of Eq. (8).

Let us consider a noisy sinusoidal signal, which is given by

$$y(t)=\ \sin(2\pi\times 0.02t)+n(t) \tag{10}$$

where $n(t)$ is a Gaussian white noise with a standard deviation of 1.5. The sampling frequency is 5 Hz, and the length of the signal is 1000. For the conventional bistable model and the new proposed model, the same model parameters a and b are used. In this simulation, a and b are respectively 1 and 2. The noisy signal is illustrated in Fig. 1. The denoised signal obtained by the conventional bistable model is illustrated in Fig. 2, while the denoised signal obtained by the new bistable model is illustrated in Fig. 3. It is easy to note from Figs. 2 and 3 that the denoised signal in Fig. 3 has less noise and is more smooth

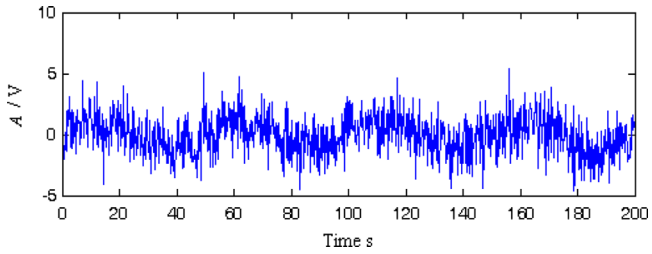

Fig. 1. The waveform of a noisy sinusoidal signal.

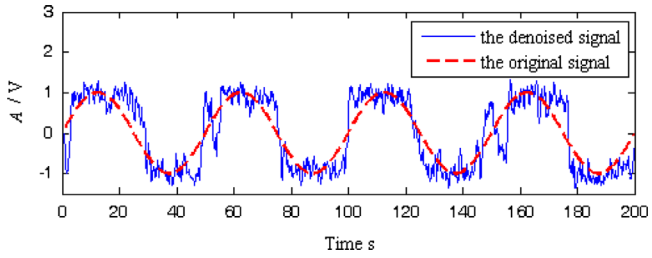

Fig. 2. The denoised result obtained by the conventional bistable model.

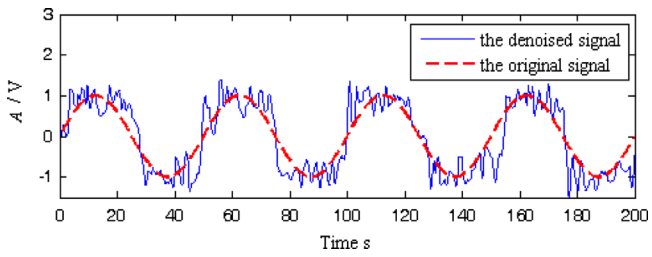

Fig. 3. The denoised result obtained by the new bistable model.

than that in Fig. 2. Moreover, the SNR of the denoised signal obtained by the conventional bistable model is 4.3 dB, while that of the denoised signal obtained by the new bistable model is 5.0 dB. The simulation results again reveal that we can get the better denoising performance by using the new bistable model due to the role of the second-order difference item.

3.2. *The adaptive iteration algorithm for implementing optimal SR*

Barrier parameters play an important role in a bistable system. To enhance the resonance effect of SR, it is necessary to research how to get optimal system parameters a and b. The traditional way is to search for the optimal system parameters in a given searching range according to the maximization of the measurement index of SR. For such a type of optimal selection approach, the measurement index should be chosen first, and then the searching range and step size need to be appropriately set in advance. Especially, the searching range of system parameters is important for an optimal searching algorithm. Setting a wide searching range, the optimal parameters can be found with more possibility. However, to increase the processing speed, the searching range is required to be narrow. Thus, how to set a suitable searching range is a key problem for the optimal system parameters searching method. Moreover, it can be seen from Figs. 2 and 3 that the output signal of SR is still interfered by part of the noise and has some glitches. Therefore, in order to further improve the calculation speed and the quality of system output, this paper proposes an adaptive iteration algorithm to get the optimal system parameters fast and obtain the desired output with high signal-to-noise ratio (SNR), by making use of dyadic wavelet transform and the least square system parameters solving method.

Wavelet transform has good time–frequency localization and filtering characteristics, and it has been widely applied to nonstationary signal processing. Particularly, compared with the commonly used discrete wavelet transform, dyadic wavelet transform is shift invariant [30], thus it demonstrates better performance in some signal processing applications, such as signal denoising and singularity detection. To remove the remaining noise and glitches in the output signal of SR based on the new bistable model, dyadic wavelet transform is used to post-process the SR output signal. Let $f(t)$ be the analyzed

signal and $f(t) \in L^2(\mathbf{R})$, the dyadic wavelet transform is defined as

$$Wf_i(\tau, 2^j) = \int_{-\infty}^{\infty} f(t) \frac{1}{\sqrt{2^j}} \psi\left(\frac{t-\tau}{2^j}\right) \mathrm{d}t = f * \overline{\psi}_{2^j}(\tau) \tag{11}$$

$$\overline{\psi}_{2^j}(t) = \psi_{2^j}(-t) = \frac{1}{\sqrt{2^j}} \psi\left(-\frac{t}{2^j}\right) \tag{12}$$

where ψ is the wavelet and $*$ denotes the operator of convolution. The dyadic wavelet transform can be implemented by à trous algorithm [31]. This algorithm can also be depicted as the cascade filter scheme, but it does not have down-sampling and up-sampling operations compared to Mallat algorithm. By means of dyadic wavelet transform, the output signal of SR is decomposed into wavelet coefficients and scale coefficients. Since noise and glitches mainly lie in wavelet coefficients, we can set the value of wavelet coefficients as zero, and then reconstruct the signal by the use of scale coefficients and the new wavelet coefficients with zero value. The reconstructed signal is more smooth and approximate to the original system input without noise.

Suppose that $s_n(t)$ is the noisy input signal which satisfies $s_n(t) = s(t) + n(t)$. Given an arbitrary bistable system, let $y'(t)$ be the SR output signal and $y(t)$ be the post-processing signal obtained by dyadic wavelet transform. We expect that the output signal is the estimate of $y(t)$ after $y(t)$ is input into a bistable system given by Eq. (8). After discretizing $y(t)$, it follows from Eq. (8) that the new system parameters can be calculated by the following equation:

$$\begin{bmatrix} a \\ b \end{bmatrix} \begin{bmatrix} \mathbf{Y} \\ -\mathbf{Y}^3 \end{bmatrix} = \mathbf{D}_2\mathbf{Y} + \mathbf{D}_1\mathbf{Y} - \mathbf{Y} \tag{13}$$

where $\mathbf{Y}$ denotes the discrete signal of $y(t)$, $\mathbf{D}_1$ and $\mathbf{D}_2$ are, respectively, the first-order differential equation and the second-order differential equation. Obviously, Eq. (13) represents an overdetermined system of equations. By means of the least square method, Eq. (13) can be solved, i.e., we can get the least square solutions of system parameters a and b. In other words, if we input $y(t)$ into the new bistable system, due to the filtering effect of the bistable system, the system output can be regarded as the estimate of $y(t)$, but SR may not be stimulated since the noise intensity is not enough. Therefore, after obtaining the updated system parameters, we input the noisy signal $s_n(t)$ into the new bistable system and SR is realized because of strong noise. By adjusting the system parameters, the SR and filtering effect is enhanced, so the new output signal will have higher SNR. In some ways, the new system output is equivalent to the filtered result of the last system output. After some iterations, the new SR output signal will be approximately in agreement with the last SR output signal. It then follows that the optimal SR detection result is obtained.

In engineering, to achieve SR, the input signal and the bistable model are usually required to be discretized. Suppose the sampling frequency is f_s and the discrete signal of $s_n(t)$ is $s_n(n)$. If the signal frequency is too large, i.e. the sampled signal parameter is too large, the SR cannot be generated, thus the re-scaling method needs to be used [19]. The steps of the adaptive SR based on the least square parameters solving method and dyadic wavelet transform are summarized as follows:

(1) Set the initial values of the system parameters a and b, and frequency-scale ratio R. a is usually set as 1, b can be set as between 0.1 and 1, and R should be chosen according to the frequency characteristic of the signal.
(2) By the use of frequency-scale ratio R, the large frequency signal is compressed linearly into the signal with small parameter frequency. Let $s_c(n)$ denote the compressed signal.
(3) Let $y_o(n)$ denote the last SR detection result signal and $y_o(n)$ can be initialized as $s_c(n)$.
(4) Using the system parameters a and b, the SR output $y'(n)$ can be calculated by Eq. (9) with the fourth-order Runge–Kutta method.
(5) Choose Daubechies wavelets with five vanishing moments, and set the decomposition stage (it is usually set to be higher than 4). Then perform dyadic wavelet transform on $y'(n)$, and obtain the wavelet coefficients and scale coefficients. Set the value of wavelet coefficients as zero, and reconstruct the signal by the use of scale coefficients and the new wavelet coefficients with zero value. Let the reconstructed signal be $y(n)$.
(6) Calculate the relative energy error between $y_o(n)$ and $y(n)$ by

$$e = \frac{\sum_n [y(n) - y_o(n)]^2}{\sum_n y_o^2(n)} \tag{14}$$

(7) Let TH denote the threshold and it can be taken as 0.08. If $e > TH$, calculate the new system parameters a and b by Eq. (13) and repeat steps (3)–(6). Otherwise, according to the frequency-scale ratio R, recover the detection result with the original large frequency parameter through $y(n)$, and then stop the iteration.

The flowchart of this proposed algorithm is illustrated in Fig. 4. With this method, the optimal weak signal detection result is usually obtained after several iterations.

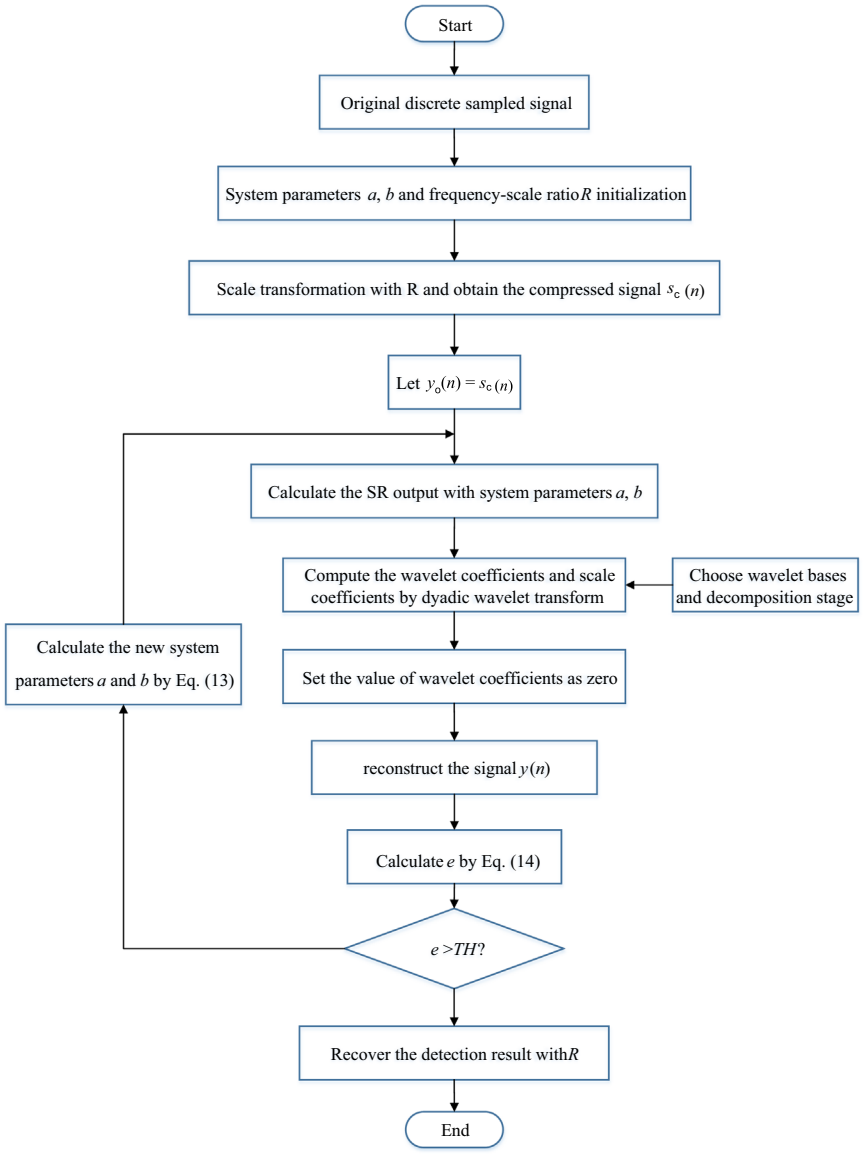

Fig. 4. The flowchart of this proposed adaptive SR method.

4. Simulation and comparison

In order to validate the effectiveness and advantage of the proposed method in this present study, two types of typical signals are selected for simulation analysis, and the commonly used weak signal detection approaches, wavelet transform and traditional adaptive SR are used for comparison.

4.1. Harmonic vibration signal analysis

Harmonic vibration is a typical vibration generated by rotatory machinery. By analyzing this type of vibration signal, we can know the running state of the machine. Let us consider the following two-component harmonic vibration signal:

$$s_n(t) = 1\ \sin(2\pi \times f_0 t) + 0.6\ \sin(2\pi \times 2f_0 t) + n(t) \tag{15}$$

where $f_0 = 3$ and $n(t)$ is Gaussian white noise with a standard deviation of 3. By calculation, the SNR of the noisy harmonic signal is -10.8577 dB. The sampling frequency is 500 Hz, and the sampling length is 2048. The original harmonic vibration signal and noisy harmonic vibration signal are respectively shown in Fig. 5(a) and (b). It is obvious that the useful vibration signal is polluted by strong noise. Thus, the proposed SR method is applied to process the noisy signal. The frequency-scale ratio R is 100, and the decomposition stage is 5. After four iterations, the optimal detection result is obtained. The natural

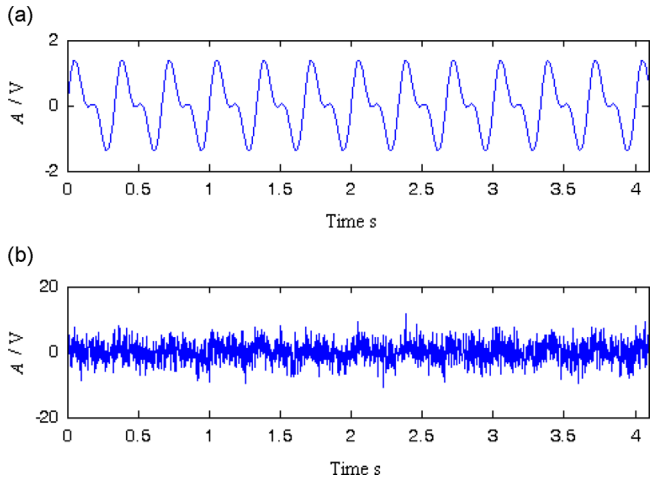

Fig. 5. Simulated vibration signals: (a) the original harmonic vibration signal and (b) the noisy harmonic vibration signal.

logarithm of e and the SNR of $y(n)$ obtained at each iteration are respectively shown in Fig. 6(a) and (b). It can be seen from Fig. 6 that this algorithm has good convergence. The optimal denoised signal and its frequency spectrum are respectively shown in Fig. 7(a) and (b). Obviously, the two-component harmonic vibration is effectively detected.

To demonstrate the advantage of the proposed method, the discrete wavelet transform and the traditional adaptive SR method based on parameter tuning are used for comparison. For the discrete wavelet transform, Daubechies wavelets with five vanishing moments are used, the decomposition stage is also 5 and the adaptive threshold selection rule uses the principle of Stein's Unbiased Risk Estimate. Fig. 8(a) and (b) respectively illustrate the denoised signal obtained by discrete wavelet transform and its frequency spectrum. For the traditional adaptive SR method based on parameter tuning, the system parameter $a=1$ is fixed, the searching range of b is [0.1, 14.9], the searching step size is 0.2, and the SNR of the detection result is used as the measurement index. Fig. 9(a) and (b) respectively illustrate the denoised signal obtained by traditional adaptive SR and its frequency spectrum. In such case, the calculation time of the traditional adaptive SR method is 284.73 s, while the calculation time of the proposed method is 8.08 s. It then follows immediately that the proposed method greatly improves the computation speed of traditional adaptive SR. By comparing Figs. 7–9, we can see that the detection results obtained by discrete wavelet transform and traditional adaptive SR still have some noise, and the detection result obtained by the proposed method is more smooth and approximate to the original harmonic vibration signal. It can also be seen from Figs. 7(b) and 8(b) that there are a large number of obvious frequency components at [10,20] Hz and other high-frequency noise in Fig. 8(b), although the spectral lines at f_0 and $2f_0$ in Fig. 8(b) are higher than those in Fig. 7(b). The SNRs obtained by the three methods are listed in Table 1. It further validates the advanced weak feature detection performance of the proposed method.

4.2. Amplitude modulated vibration signal analysis

If a rub-impact fault occurs in a rotor system, the impact may cause the vibration modulation phenomenon. By extracting the modulation characteristics, the rub-impact fault can be effectively identified. Let us consider an amplitude modulated vibration signal

$$s_n(t)=(1+0.4\ \cos\ 2\pi f_1 t)\sin(2\pi\times f_0 t)+0.6(1+0.4\ \cos\ 2\pi f_1 t)\sin(2\pi\times 2f_0 t)+n(t) \tag{16}$$

where $f_0=0.02$, $f_1=0.002$ and $n(t)$ is Gaussian white noise with a standard deviation of 3.8. By calculation, the SNR of the noisy amplitude modulated signal is -13.4589 dB. The sampling frequency is 5 Hz, and the sampling length is 2048. The original amplitude modulated vibration signal and noisy amplitude modulated vibration signal are respectively shown in Fig. 10(a) and (b). The proposed SR method is applied to processing the noisy amplitude modulated signal. The frequency-scale ratio R is 1, and the decomposition stage is 6. After five iterations, the optimal detection result is obtained. The natural logarithm of e and the SNR of $y(n)$ obtained at each iteration are respectively shown in Fig. 11(a) and (b). Fig. 11 validates the good convergence of the proposed method again. The optimal denoised signal and its frequency spectrum are respectively shown in Fig. 12(a) and (b). Obviously, the two-component amplitude modulated vibration is effectively detected.

Similarly, both the discrete wavelet transform and the traditional adaptive SR method based on parameter tuning are used to process the same signal. For the discrete wavelet transform, Daubechies wavelets with five vanishing moments are used, the decomposition stage is 6 and the adaptive threshold selection rule uses the principle of Stein's Unbiased Risk Estimate. Fig. 13(a) and (b) respectively illustrate the denoised signal obtained by discrete wavelet transform and its frequency spectrum. For the traditional adaptive SR method based on parameter tuning, the system parameter $a=1$ is also fixed, the searching range of b is also [0.1, 14.9], the searching step size is also 0.2, and the SNR of the detection result is used

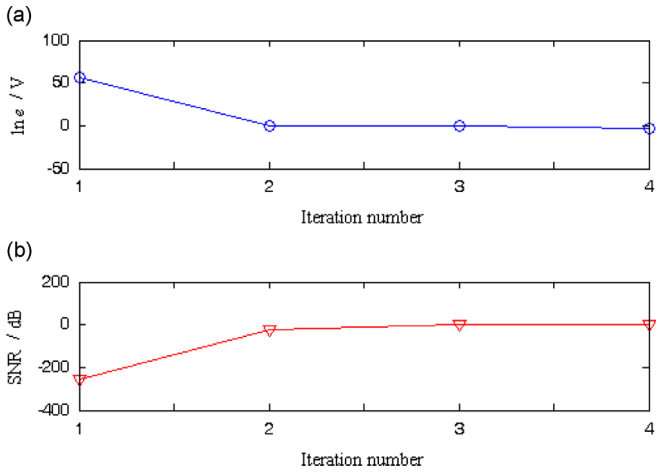

Fig. 6. Evaluation index at each iteration for noisy harmonic signal: (a) the natural logarithm of e and (b) the SNR of $y(n)$.

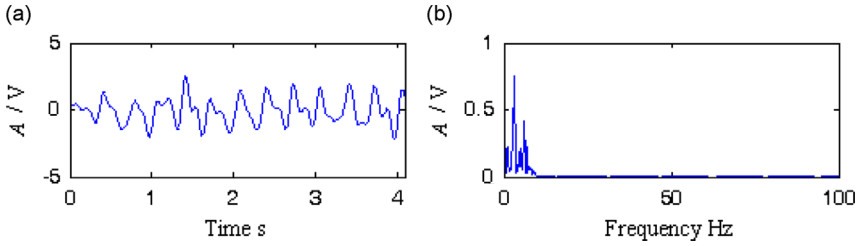

Fig. 7. The detection result of noisy harmonic vibration signal obtained by the proposed method: (a) the denoised signal and (b) its frequency spectrum.

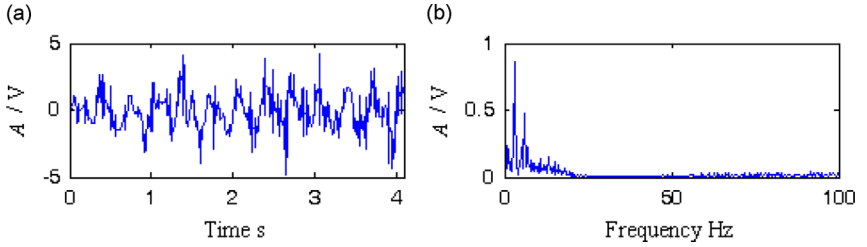

Fig. 8. The detection result of noisy harmonic vibration signal obtained by discrete wavelet transform: (a) the denoised signal and (b) its frequency spectrum.

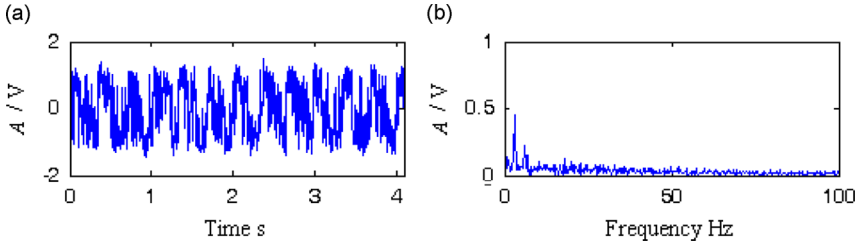

Fig. 9. The detection result noisy harmonic vibration signal obtained by traditional adaptive SR: (a) the denoised signal and (b) its frequency spectrum.

Table 1
The SNRs of denoised harmonic vibration signals obtained by three methods.

Method	The proposed method	Discrete wavelet transform	Traditional adaptive SR
SNR	2.3654	1.2087	1.6392

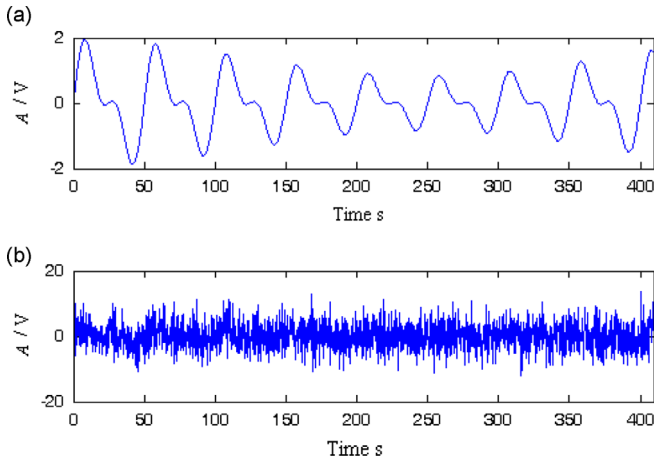

Fig. 10. Simulated vibration signals: (a) the original amplitude modulated vibration signal and (b) the noisy amplitude modulated vibration signal.

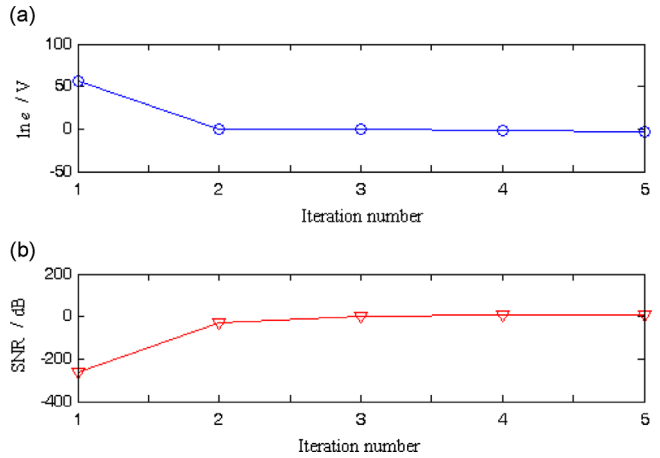

Fig. 11. Evaluation index at each iteration for noisy amplitude modulated signal: (a) the natural logarithm of e and (b) the SNR of $y(n)$.

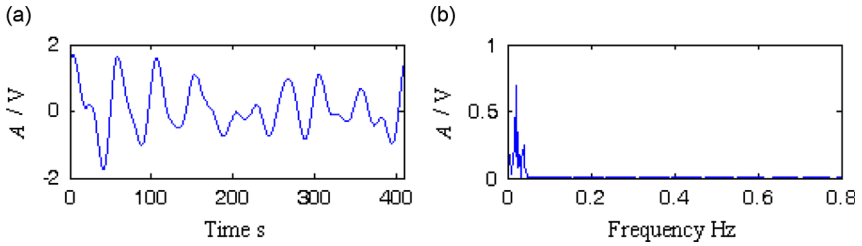

Fig. 12. The detection result of noisy amplitude modulated vibration signal obtained by the proposed method: (a) the denoised signal and (b) its frequency spectrum.

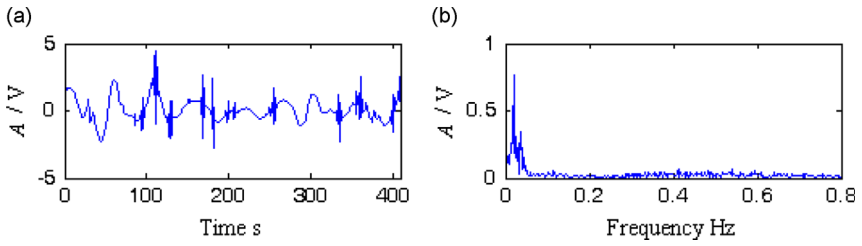

Fig. 13. The detection result of noisy amplitude modulated vibration signal obtained by discrete wavelet transform: (a) the denoised signal and (b) its frequency spectrum.

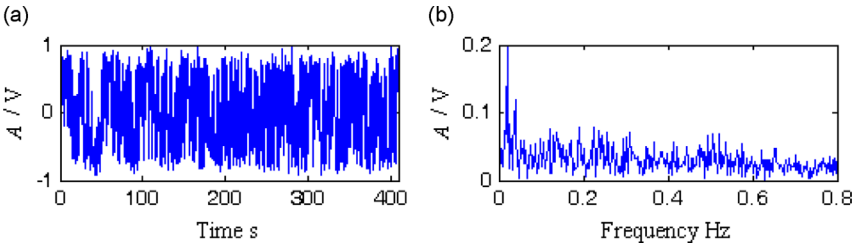

Fig. 14. The detection result noisy amplitude modulated vibration signal obtained by traditional adaptive SR: (a) the denoised signal and (b) its frequency spectrum.

Table 2
The SNRs of denoised amplitude modulated vibration signals obtained by three methods.

Method	The proposed method	Discrete wavelet transform	Traditional adaptive SR
SNR	4.7076	2.6568	0.2210

as the measurement index. Fig. 14(a) and (b) respectively illustrate the denoised signal obtained by traditional adaptive SR and its frequency spectrum. In this simulation experiment, the calculation time of the traditional adaptive SR method is 315.80 s, while the calculation time of the proposed method is 11.37 s. It again demonstrates that the proposed method has a much higher computation speed. By comparing Figs. 12–14, we can see that the detection result obtained by traditional adaptive SR is still seriously interfered by noise, the detection result obtained by discrete wavelet transform has some clear impact, and the detection result obtained by the proposed method is more smooth and approximate to the original amplitude modulated vibration signal. Furthermore, comparing Fig. 12(b) with Fig. 13(b), we can see that the frequency spectrum in Fig. 13(b) is disturbed by high frequency components while the frequency spectrum in Fig. 12(b) does not have these high frequency interferences. The SNRs obtained by the three methods are listed in Table 2. It can be seen that the proposed method has the best weak signal detection performance.

5. Application into mechanical fault feature extraction

To validate the feasibility of the proposed method in mechanical engineering application, it is used to detect the fault of a rotor system. A rotor test rig is established, and its schematic sketch is illustrated in Fig. 15. The test rig mainly includes an alternating current (AC) servo motor, a shaft coupling, two rolling bearings and a rotor. An eddy current sensor is used to acquire the vibration displacement signal of the spindle. To increase the noise intensity in the sampled signal, the electromagnetic interference is imposed on the measuring circuit of the vibration displacement signal. And a photoelectric tachometric transducer is used to measure the rotating speed of the spindle.

Firstly, a rotor with a crack is used. In this experiment, a cut at the root of the rotor is processed by the wire cutting machine, and then a fatigue test equipment is used to produce the crack. The dimensions of the crack fault are 4 mm depth and 20 mm length. When the rotor has a crack, the vibration signal will contain obvious double rotating frequency component except for the rotating frequency component. In the experiment, the rotating frequency of the spindle f_r is 30.1218 Hz. To well motivate the SR phenomenon, a large sampling frequency is chosen as 8000 Hz, and the length of sampling data is 4096. The time domain waveform of the sampled vibration displacement signal and its frequency spectrum are respectively shown in Fig. 16(a) and (b). From Fig. 16(b), we can see that there is a clear spectral line at f_r, whereas there is no clear spectral line at $2f_r$ due to the noise. Consequently, the proposed method is applied to extracting the crack fault feature. The frequency-scale ratio R is 800, and the decomposition stage is 6. The detection result is obtained via four iterations, whose time domain waveform and frequency spectrum are respectively shown in Fig. 17(a) and (b). It can be seen from Fig. 17(b) that there are two clear spectral lines at f_r and $2f_r$. It follows that there is a crack fault in the rotor.

Like the simulation, the discrete wavelet transform and the traditional adaptive SR method based on parameter tuning are used for comparison. With the same wavelets, decomposition stage and threshold selection rule in Section 4.2, the detection result obtained by the discrete wavelet transform is illustrated in Fig. 18. It can be seen from Fig. 18(a) that most of the noise is removed. However, there is no clear spectral line at the fault characteristic frequency $2f_r$ in Fig. 18(b). For the traditional adaptive SR method, the system parameter $a = 1$ is also fixed, the searching range of b is $[0.1,\ 14.9]$, the searching step size is also 0.2, and the amplitude at the fault characteristic frequency is used as the measurement index. Fig. 19(a) and (b) respectively illustrate the denoised signal and its frequency spectrum obtained by traditional adaptive SR. From this figure, we can see that the detection result still has some noise and there is no clear spectral line at the fault characteristic frequency $2f_r$. Moreover, the computation time of traditional adaptive SR is up to 683.5 s, while the computation time of the proposed method is 17.2 s. Therefore, the proposed method is superior to the traditional adaptive SR in both weak signal detection performance and computational complexity.

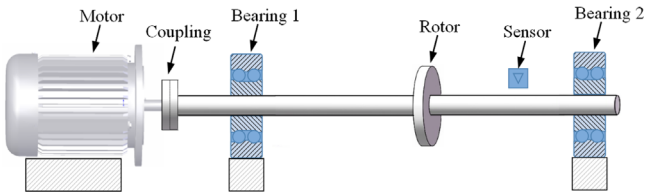

Fig. 15. The schematic sketch of a rotor test rig.

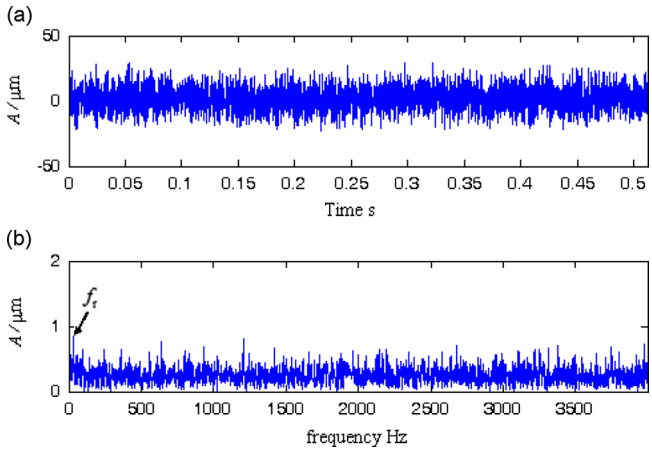

Fig. 16. The crack fault vibration signal of a rotor system and its frequency spectrum: (a) time domain waveform and (b) frequency spectrum.

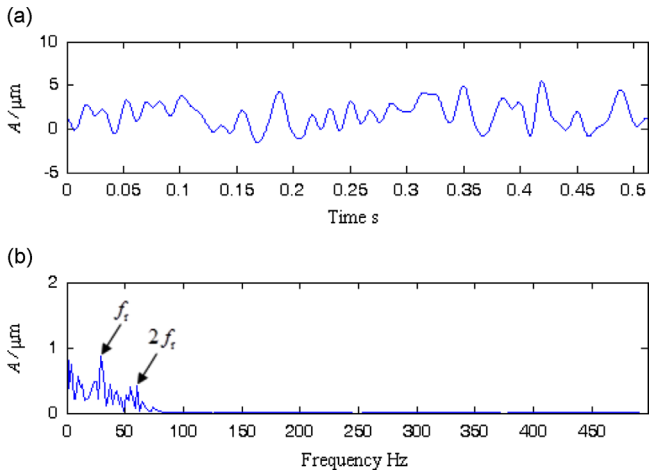

Fig. 17. The detection result of the crack fault vibration signal obtained by the proposed method: (a) time domain waveform and (b) frequency spectrum.

Secondly, a rotor with eccentric mass is used for the experiment. In such case, rotor unbalance fault will occur, and the vibration signal not only has a large rotating frequency component, but also small higher harmonics of the rotating frequency component. The rotating frequency of the spindle f_r is 89.6853 Hz, the sampling frequency is chosen as 40 kHz, and the length of sampling data is 10,240. The time domain waveform of the sampled vibration displacement signal and its frequency spectrum are respectively shown in Fig. 20(a) and (b). It can be seen from Fig. 20 that the useful vibration components are submerged in strong noise and there are no spectral lines at frequency multiplication of the rotating frequency. Thus, the proposed method is applied to extract the unbalance fault feature. The frequency-scale ratio R is 4000, and the decomposition stage is 6. After five iterations, the optimal detection result is obtained, whose time domain waveform and frequency spectrum are respectively shown in Fig. 21(a) and (b). It can be seen from Fig. 21 that there are two peaks at $2f_r$ and $3f_r$, whose values are much smaller than the amplitude at f_r. It follows that there is an unbalance fault. Similarly, with the same wavelets, decomposition stage and threshold selection rule, the denoised signal and its frequency spectrum obtained by the discrete wavelet transform are respectively illustrated in Fig. 22(a) and (b). We can see that the denoised signal has a lot of impact and the spectral line at $3f_r$ is not obvious. The traditional adaptive SR method is also

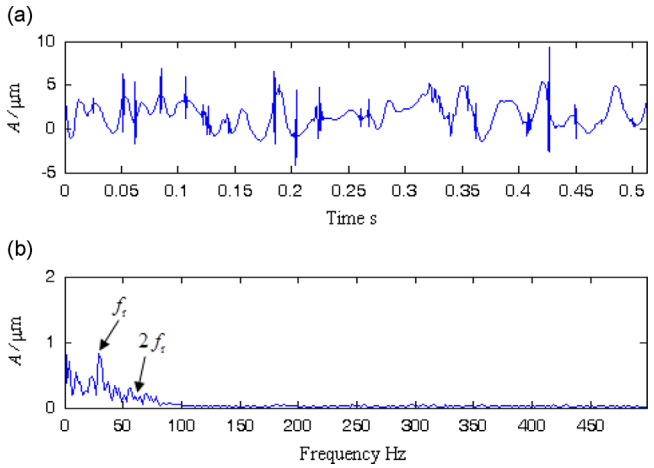

Fig. 18. The detection result of the crack fault vibration signal obtained by discrete wavelet transform: (a) time domain waveform and (b) frequency spectrum.

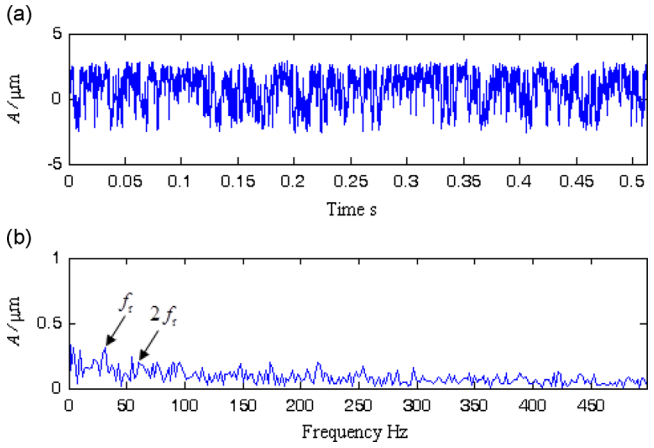

Fig. 19. The detection result of the crack fault vibration signal obtained by traditional adaptive SR: (a) time domain waveform and (b) frequency spectrum.

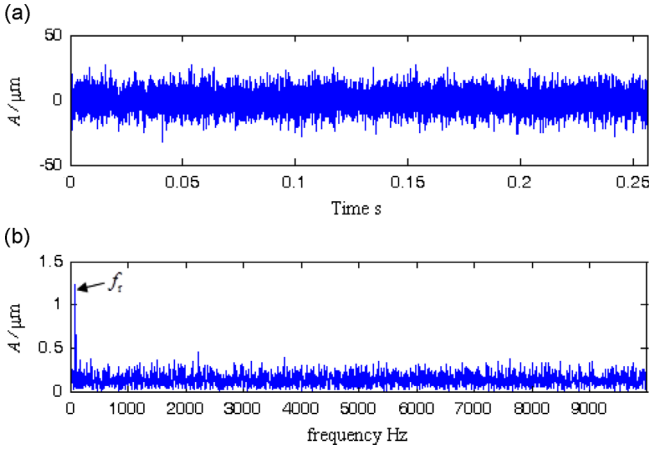

Fig. 20. The unbalance fault vibration signal of a rotor system and its frequency spectrum: (a) time domain waveform and (b) frequency spectrum.

employed to analyze the same vibration signal. Fig. 23(a) and (b) respectively illustrate the detection result and its frequency spectrum obtained by traditional adaptive SR with the same parameter setup and the measurement index used in the last experiment. We can see from Fig. 23 that the detection result is still seriously interfered by noise and the spectral line at $3f_r$

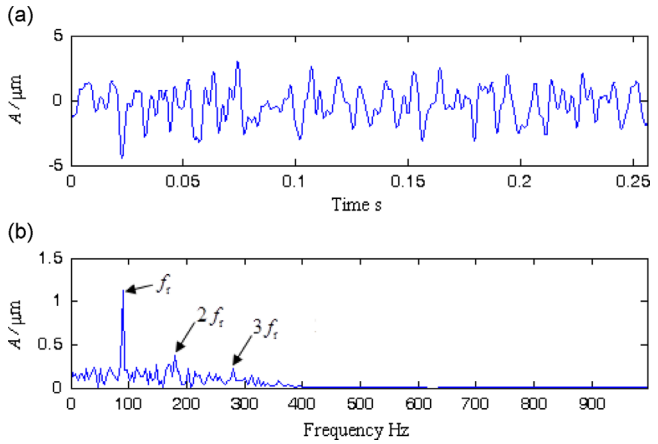

Fig. 21. The detection result of the unbalance fault vibration signal obtained by the proposed method: (a) time domain waveform and (b) frequency spectrum.

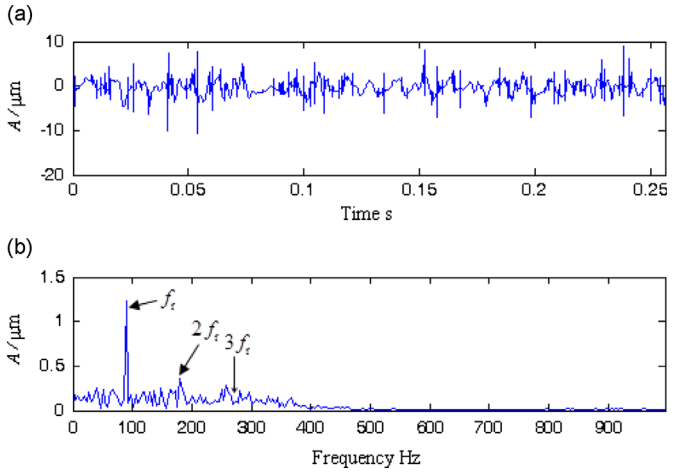

Fig. 22. The detection result of the unbalance fault vibration signal obtained by discrete wavelet transform: (a) time domain waveform and (b) frequency spectrum.

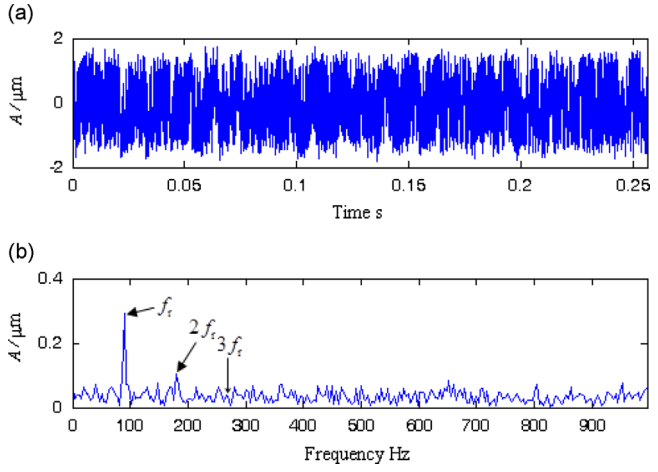

Fig. 23. The detection result of the unbalance fault vibration signal obtained by traditional adaptive SR: (a) time domain waveform and (b) frequency spectrum.

is also not obvious. Furthermore, the computational complexity of traditional adaptive SR is very high, and its computation time is up to 2215.3 s, whereas the computation time of the proposed method is just 77.3 s. This experiment further demonstrates the superiority of the proposed method to discrete wavelet transform and the traditional adaptive SR method.

6. Conclusions

An adaptive and fast SR approach is introduced in this paper. A new bistable model with both a first-order differential item and a second-order differential item is set up and used in the proposed adaptive SR method. This model can further increase the noise utilization and improve the quality of SR output. As the output of SR is not smooth and still has some noise, wavelet transform is employed to post-process the output signal, and the smoothed vibration signal can be obtained. Except for the Daubechies wavelets with five vanishing moments used in this paper, other wavelets can be used for wavelet transform. To increase the calculation speed and improve the weak feature detection performance, an adaptive iteration algorithm for implementing optimal SR based on wavelet transform and system parameters solving is proposed in this present study. Compared with the traditional adaptive SR method, the proposed algorithm can get optimal detection result via a few iterations, thus its computation complexity is lower, whereas the computation complexity of traditional adaptive SR mainly depends on the searching range and searching step size, and a large number of iterations are usually required.

This proposed method, discrete wavelet transform and traditional adaptive SR are applied to the simulation experiments and practical application. The results show that this proposed method has the best weak feature detection performance. Therefore, it can be concluded that the proposed method has great potential in various engineering fields.

Acknowledgments

The work described in this paper was supported by the Fundamental Research Funds for the Central Universities (No. CDJZR14285501), China Postdoctoral Science Foundation funded project (No. 2012M521690), Natural Science Foundation Project of CQ CSTC (cstc2012jjA70003), and National Natural Science Foundation of China (No. 51005262).

References

[1] B.Q Chen, Z.S. Zhang, C. Sun, B. Li, Y.Y. Zi, Z.J. He, Fault feature extraction of gearbox by using overcomplete rational dilation discrete wavelet transform on signals measured from vibration sensors, *Mechanical Systems and Signal Processing* 33 (2012) 275–298.
[2] Y. Qin, J.X. Wang, Y.F. Mao, Dense framelets with two generators and their application in mechanical fault diagnosis, *Mechanical Systems and Signal Processing* 40 (2) (2013) 483–498.
[3] Y. Qin, Y.F. Mao, B.P. Tang, Vibration signal component separation by iteratively using basis pursuit and its application in mechanical fault detection, *Journal of Sound and Vibration* 332 (20) (2013) 5217–5235.
[4] Xuefeng Chen Gaigai Cai, Zhengjia He. Sparsity-enabled signal decomposition using tunable Q-factor wavelet transform for fault feature extraction of gearbox, *Mechanical Systems and Signal Processing* 41 (1–2) (2013) 34–53.
[5] Y.G. Lei, J. Lin, Z.J. He, M.J. Zuo, A review on empirical mode decomposition in fault diagnosis of rotating machinery: review article, *Mechanical Systems and Signal Processing* 35 (1–2) (2013) 108–126.
[6] M. Zvokelj, S. Zupan, I. Prebil, Non-linear multivariate and multiscale monitoring and signal denoising strategy using kernel principal component analysis combined with ensemble empirical mode decomposition method, *Mechanical Systems and Signal Processing* 25 (7) (2011) 2631–2653.
[7] Y. Qin, Multicomponent AM–FM demodulation based on energy separation and adaptive filtering, *Mechanical Systems and Signal Processing* 38 (2) (2013) 440–459.
[8] N.Q. Hu, M. Chen, X.S. Wen, The application of stochastic resonance theory for early detecting rub-impact fault of rotor system, *Mechanical Systems and Signal Processing* 17 (4) (2003) 883–895.
[9] Y.G. Lei, D. Han, J. Lin, Z.J. He, Planetary gearbox fault diagnosis using an adaptive stochastic resonance method, *Mechanical Systems and Signal Processing* 38 (1) (2013) 113–124.
[10] S.L. Lu, Q.B. He, F.R. Kong, Stochastic resonance with Woods–Saxon potential for rolling element bearing fault diagnosis, *Mechanical Systems and Signal Processing* 45 (2) (2014) 488–503.
[11] T. Oya, T. Asai, Y. Amemiya, Stochastic resonance in an ensemble of single-electron neuromorphic devices and its application to competitive neural networks, *Chaos, Solitons and Fractals* 32 (2) (2014) 855–861.
[12] R. Benzi, A. Sutera, A Vulpiana, The mechanism of stochastic resonance, *Journal of Physics A: Mathematical and General* 14 (11) (1981) 453–457.
[13] S. Fauve, F Heslot, Stochastic resonance in a bistable system, *Physics Letters A* 97 (1–2) (1983) 5–7.
[14] V.S Anishchenko, M.A. Safonova, L.O. Chua, Stochastic resonance in Chua's circuit, *International Journal of Bifurcation and Chaos* 2 (2) (1992) 397–401.
[15] B. McNamara, K. Wiesenfield, R. Roy, Observation of stochastic resonance in a ring laser, *Physical Review Letters* 60 (25) (1988) 2626–2629.
[16] H. Gang, G. Nicolis, C. Nicolis, Periodically forced Fokker–Planck equation and stochastic resonance, *Physical Review A* 42 (4) (1990) 2030–2041.
[17] L. Gammaitoni, P. Hanggi, P. Jung, F. Marchesoni, Stochastic resonance, *Reviews of Modern Physics* 70 (1) (1998) 223–287.
[18] Y.G. Leng, T.Y. Wang, Numerical research of twice sampling stochastic resonance for the detection of a weak signal submerged in heavy noise, *Acta Physica Sinica* 52 (10) (2003) 2432–2438.
[19] Y.G. Leng, Y.S. Leng, T.Y. Wang, Y. Guo, Numerical analysis and engineering application of large parameter stochastic resonance, *Journal of Sound and Vibration* 292 (3–5) (2006) 788–801.
[20] Q. Mao, M. Lin, Y. Zheng, Study of weak multi-frequencies signal detection based on stochastic resonance, *Journal of Basic Science and Engineering* 16 (1) (2008) 86–91.
[21] J.Y Tan, X.F Chen, J.Y Wang, H.X Chen, H.R Cao, Y.Y Zi, Z.J He, Study of frequency-shifted and re-scaling stochastic resonance and its application to fault diagnosis, *Mechanical Systems and Signal Processing* 23 (3) (2009) 811–822.
[22] Q.B. He, J. Wang, Y.B. Liu, D.Y. Dai, F.R. Kong, Multiscale noise tuning of stochastic resonance for enhanced fault diagnosis in rotating machines, *Mechanical Systems and Signal Processing* 28 (2012) 443–457.
[23] V. Kohar, K. Murali, S. Sinh, Enhanced logical stochastic resonance under periodic forcing, *Communications in Nonlinear Science and Numerical Simulation* 19 (8) (2014) 2866–2873.

[24] J.M. Li, X.F. Chen, Z.J. He, Adaptive stochastic resonance method for impact signal detection based on sliding window, *Mechanical Systems and Signal Processing* 332 (22) (2013) 5999–6015.
[25] Z.Y. Lu, T.Y. Yang, M. Zhu, Study of the method of multi-frequency signal detection based on the adaptive stochastic resonance, *Abstract and Applied Analysis* (2013) 420605.
[26] H.F. Li, R.H. Bao, B.H. Xu, J.Y. Zheng, Intrawell stochastic resonance of bistable system, *Journal of Sound and Vibration* 272 (1–2) (2004) 155–167.
[27] J.M. Li, X.F. Chen, Z.J. He, Multi-stable stochastic resonance and its application research on mechanical fault diagnosis, *Journal of Sound and Vibration* 292 (3–5) (2006) 788–801.
[28] R.L. Harne, M. Thota, K.W. Wang, Concise and high-fidelity predictive criteria for maximizing performance and robustness of bistable energy harvesters, *Applied Physics Letters* 102 (5) (2013) 053903.
[29] R.L. Harne, K.W. Wang, Robust sensing methodology for detecting change with bistable circuitry dynamics tailoring, *Applied Physics Letters* 102 (20) (2013) 203506.
[30] S. Mallat, *A Wavelet Tour of Signal Processing*, Academic Press, San Diego, 1999.
[31] M.J. Shensa, The discrete wavelet transform: wedding the à trous and Mallat algorithms, *IEEE Transactions on Signal Processing* 40 (10) (1992) 2464–2482.